J. Fluid Mech. (1986), *vol.* 171, *pp.* 547–562
Printed in Great Britain

Measurement of wall shear stress in turbulent boundary layers subject to strong pressure gradients

By F. HIRT† AND H. THOMANN
Institut für Aerodynamik, Swiss Federal Institute of Technology, Zurich, Switzerland

(Received 15 July 1985 and in revised form 20 April 1986)

Measurements of the wall shear stress with a floating element and with Preston tubes were conducted in turbulent boundary layers. Sudden application and removal of adverse pressure gradients resulted in boundary layers far from equilibrium. Positive and negative errors of the Preston-tube results were observed for adverse pressure gradients. The negative errors occurred mainly in regions with $\mathrm{d}\tau_w/\mathrm{d}x > 0$. The relation between the error, the pressure gradient and the tube size (1.1) suggested by Frei & Thomann (1980) predicts only positive errors for $\mathrm{d}p/\mathrm{d}x > 0$. Therefore, it cannot be used for the present pressure distributions and is not as general as was expected. The present results show that indirect methods to determine the wall shear stress should not extend beyond $y^+ = 3$ if accuracies of $\pm 1\,\%$ are required for pressure distributions similar to the ones used in the present investigation. Predictions from Ludwieg & Tillmann's relation (4.21) agree to within $\pm 10\,\%$ with the present measurements. The Preston-tube readings indicate velocities below the law of the wall in regions with a decreasing adverse pressure gradient. No local parameters could be found that correlated the errors of the Preston-tube results for the large pressure gradients used in the present investigation.

1. Introduction

Frei & Thomann (1980, hereinafter referred to as (I)) reported skin-friction measurements in large adverse pressure gradients. They used a floating-element balance, the gap of which was sealed with a liquid. The results were used to calibrate Preston tubes in an adverse pressure gradient. They were presented as $\tau_p - \tau_w$, where τ_p is the wall shear stress determined with the Preston tube using the calibration curve for $\mathrm{d}p/\mathrm{d}x = 0$ and τ_w is the shear stress determined with the floating element. The following relation was suggested:

$$\frac{\tau_p - \tau_w}{\tau_w} = 0.0968 \left(\frac{\nu}{\rho u_\tau^3} \frac{\mathrm{d}p}{\mathrm{d}x} \right)^{1.337} \left(\frac{u_\tau d}{\nu} \right)^{0.857}, \tag{1.1}$$

where ρ, ν and d are the density, the kinematic viscosity and the diameter of the Preston tube respectively, and $u_\tau = (\tau_w/\rho)^{\frac{1}{2}}$. Equation (1.1) is based on the often-used assumption that the flow close to the wall depends on local quantities only. It was suggested in (I) that the upstream history could be taken into account by writing $p(x)$ as a Taylor series in x and neglecting the terms with the higher p-derivatives. Equation (1.1) is based on results using two pressure distributions, one with a

† Present address: Eidgenössisches Flugzeugwerk Emmen, CH-6032 Emmen, Switzerland.

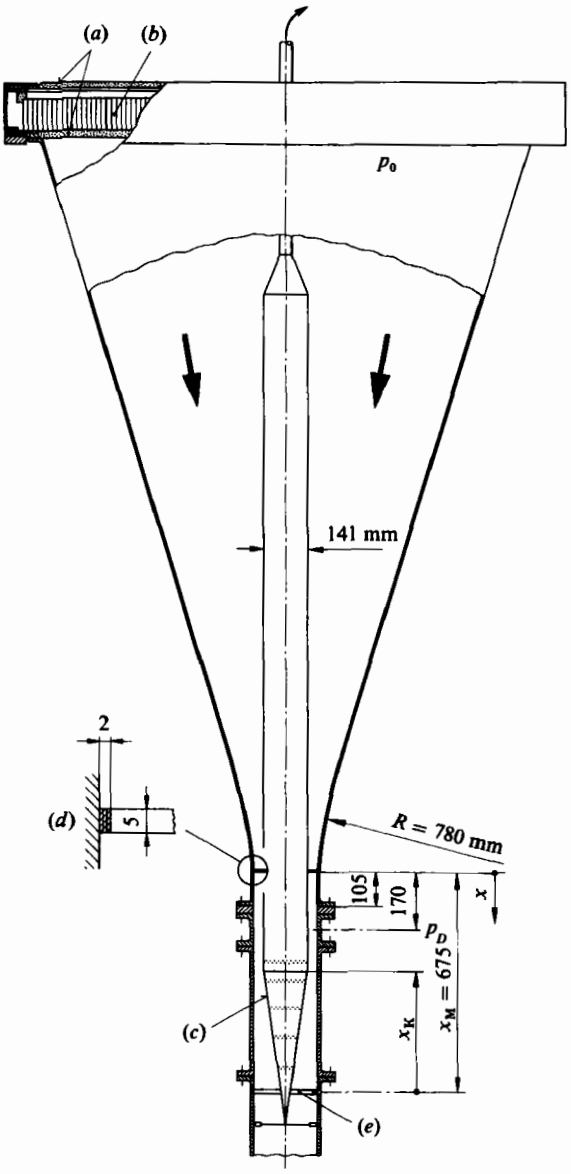

FIGURE 1. Test section: (*a*) filters; (*b*) honeycomb; (*c*) centrebody with suction; (*d*) boundary-layer trip; (*e*) location of floating element.

positive second derivative and one with a mainly negative one. As both sets of results agreed with (1.1) it was expected that the influence of the second derivative would be small. Further experiments were conducted by Hirt (1984) to test this hypothesis. The results showed that the entire upstream history of the boundary layer can have a significant influence for $d^+ = u_\tau d/\nu$ as low as 10, which means that (1.1) is not as general as expected.

It is generally agreed that a universal law of the wall $u/u_\tau = fn\ (u_\tau y/\nu)$ leads to a universal calibration curve for the Preston tube. The Preston tube can therefore be used as a convenient check of the law of the wall. The results to be presented here

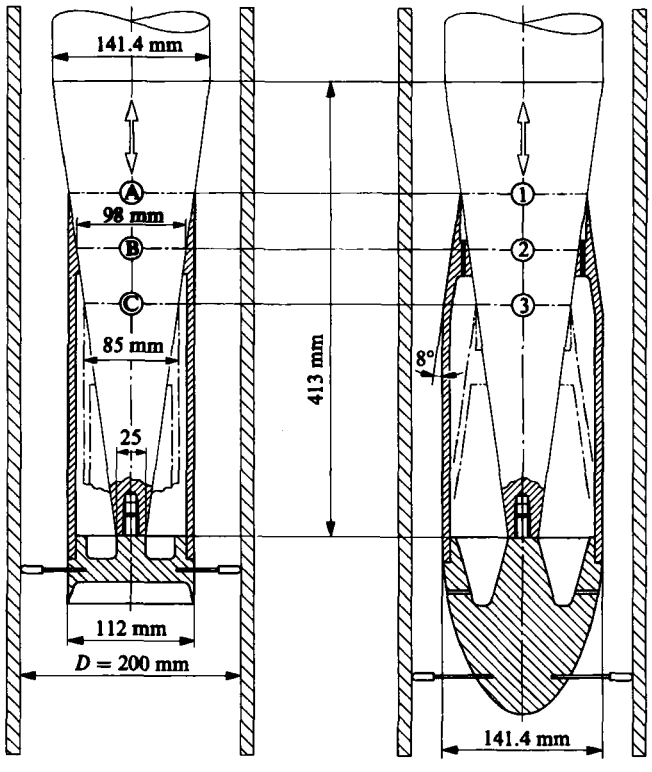

FIGURE 2. Centrebody with inserts (1)–(3) and (A)–(C).

show that the law of the wall needs corrections for $u_\tau y/\nu > 3$. For $\mathrm{d}p/\mathrm{d}x > 0$ these corrections can be positive or negative. The negative corrections for positive and vanishing $\mathrm{d}p/\mathrm{d}x$ show that the upstream history is more important than was expected by Patel (1965) and by Brown & Joubert (1969) who predict positive corrections for positive $\mathrm{d}p/\mathrm{d}x$.

2. Experimental arrangement

Few changes were made to the experimental set-up described in (I). The inlet was redesigned without the concave parts of the contour (figure 1) to prevent the formation of Görtler vortices. This change improved the uniformity of the flow somewhat. Frei's balance (figure 1 of (I)) was used with minor changes, the most important being the replacement of the floating-element ring with a new one of nominally the same dimensions. Tests with the new ring reproduced the result shown in figure 12 of (I) very well, leading to the conclusion that the geometric accuracy of the two rings was sufficient. Preston tubes with outer diameters $d = 4, 3, 2, 1$ and 0.5 mm and with a diameter ratio of 0.6 were used. The Preston-tube readings upstream of the pressure rise showed an r.m.s.-variation of 1.1 % in the circumferential direction followed by the usual increase in the region with rising pressure. Therefore, they had to be integrated along the circumference of the test section to give values that could be compared with the results of the balance. The integration was carried out by adding 36 readings taken at 10° intervals.

The different pressure distributions were generated by placing inserts on Frei's

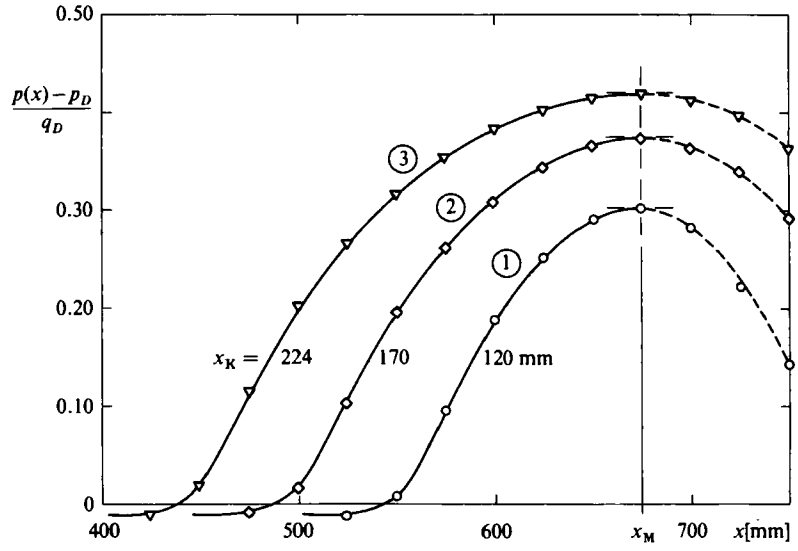

FIGURE 3. Pressure distributions with inserts (1), (2) and (3). $q_D = p_0 - p_D = 1000$ N/m², see figure 1 for p_0 and p_D.

original centrebody. The geometry of these inserts is given in figure 2. Due to the stronger boundary-layer trip used by Hirt, the turbulent boundary layer was somewhat thicker than Frei's and the inserts decreased the distance between the centrebody and the wall. This resulted in a limited core region with undisturbed mean flow between the two boundary layers. However, hot-wire measurements conducted towards the end of the investigation showed considerable turbulent fluctuations (up to 7 %) in some parts of this core region. As the Preston tubes are in a region close to the wall ($d^+ = u_\tau d/\nu < 300$), it is unlikely that these fluctuations should have a direct influence on the presented results. If this were not the case, the errors in figure 8 would not vanish upstream and downstream of the pressure rise (at $x_K = -80$ mm, not shown, and at $x_K = 350$ mm). The same argument also allows the influence of the curvature of the pipe wall on the Preston-tube reading to be neglected.

3. Results

The hypothesis that the influence of the second derivative $\mathrm{d}^2p/\mathrm{d}x^2$ on the calibration of Preston tubes should be small was tested in a first series of experiments. Inserts (1), (2) and (3) generated pressure distributions with a maximum as shown in figure 3. Measurements with the balance and with the Preston tubes were conducted at $x_M = 675$ mm, where $\mathrm{d}p/\mathrm{d}x = 0$ and $\mathrm{d}^2p/\mathrm{d}x^2 < 0$. The results are presented in figure 4. They show large negative errors of the Preston-tube readings for d^+ as low as 10, while (1.1) predicts vanishing errors as $\mathrm{d}p/\mathrm{d}x = 0$.

This unexpected behaviour gave rise to a second set of experiments in which the development of the boundary layer was investigated. The pressure distributions generated by Inserts (A)–(C) are shown in figure 5 for different positions x_K of the inserts. The wall shear stress is presented in figure 6. It should be kept in mind that figure 6 does not show the distribution of τ_w in a real boundary layer as the position of the balance remained fixed at x_M while the inserts were moved. The length with

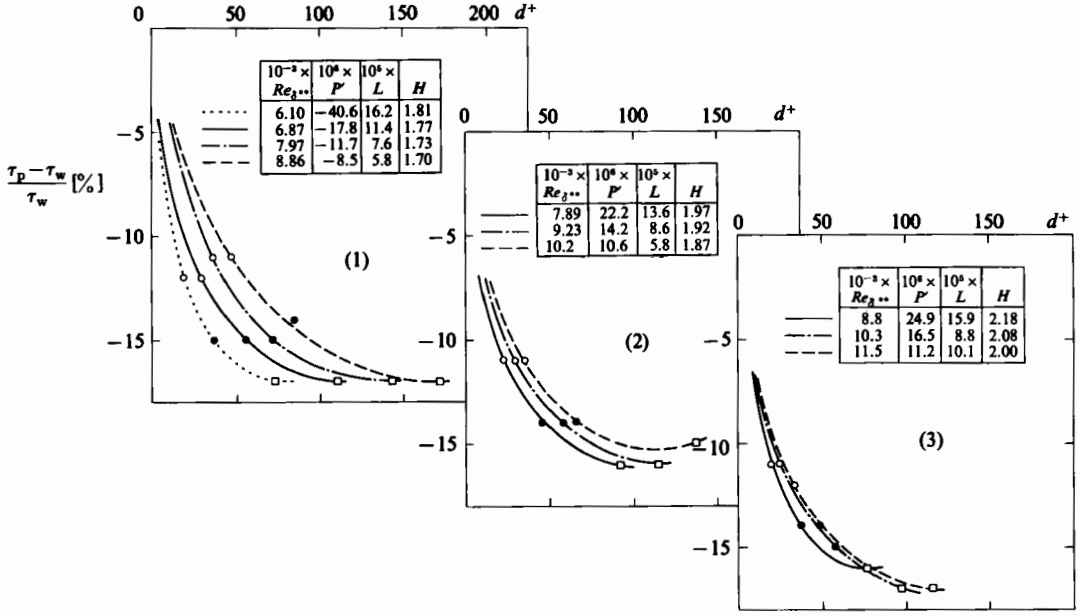

FIGURE 4. Errors of Preston-tube readings at $dp/dx = 0$ with inserts (1), (2) and (3). ------, $q_D = 500$ N/m²; ——, 1000 N/m²; — · —, 1500 N/m²; – – –, 2000 N/m². ○, $d = 0.5$ mm; ●, 1 mm; □, 2 mm.

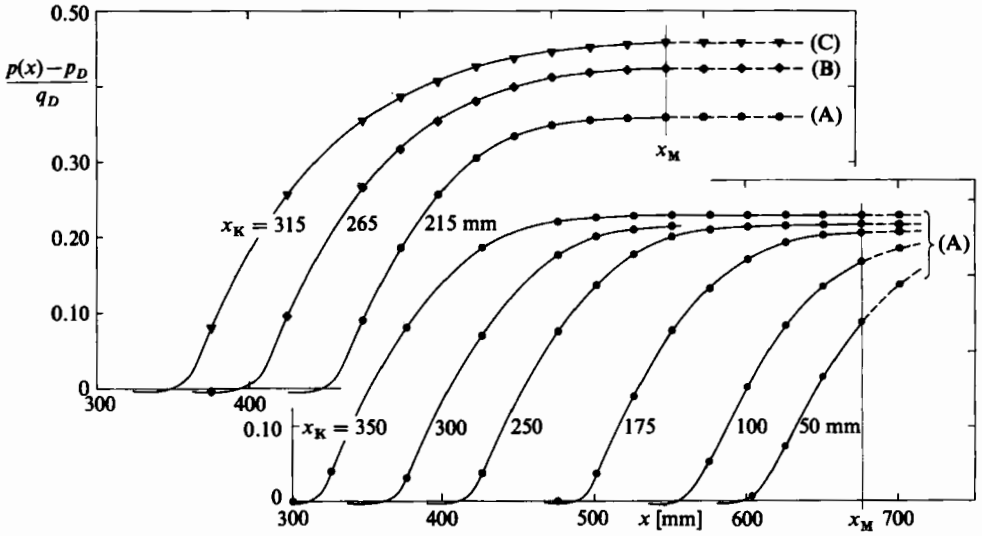

FIGURE 5. Pressure distributions with inserts (A)–(C), $q_D = 1000$ N/m².

constant area ($x_M - x_K$ in figure 1) was thus changed and with it the upstream history of the boundary layer, but the difference between τ_w (x_K) shown in figure 6 and $\tau_w(x)$ is not significant. The errors of the Preston tubes for $dp/dx = 0$ and $d^2p/dx^2 = 0$ are presented in figure 7. They show a maximum at $d^+ \approx 100$ and are comparable with the results of figure 4. Therefore, the hope of finding a relation between the error $\tau_p - \tau_w$ and local quantities based on $p(x)$ cannot be realized at this station. All these

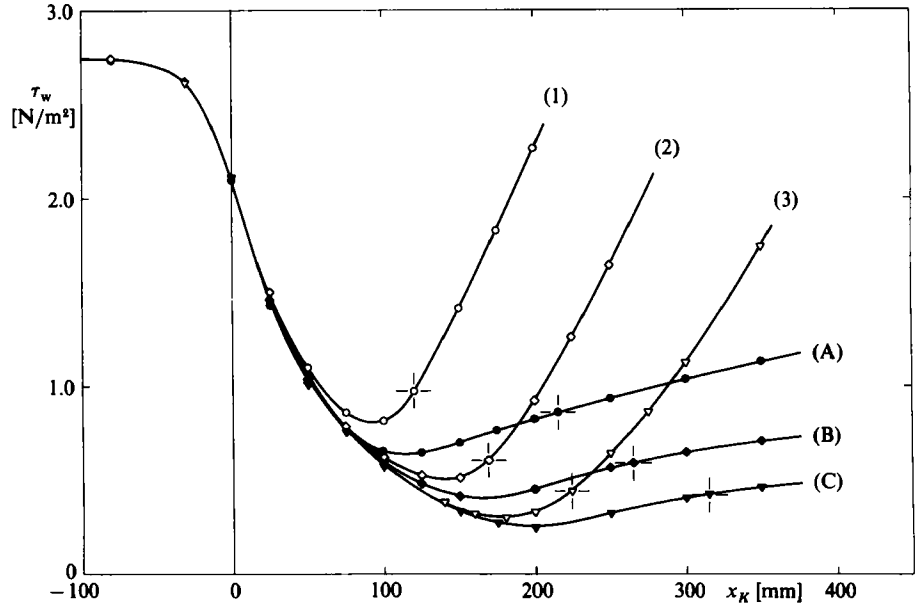

FIGURE 6. Wall shear stress at $x_M = 675$ mm for different locations x_K of the inserts, $q_D = 1000$ N/m².

experiments were conducted in regions where the boundary layer had recovered from the influence of the pressure gradient which led to $d\tau_w/dx > 0$ as shown in figure 6.

The development of the errors along the boundary layer is given in figure 8. At $x_K = 50$ mm the Preston tube overestimates the wall shear stress and the results are well described by (1.1). This was to be expected as the pressure distribution up to this station was similar to the one used in (I). A decrease of the pressure gradient leads to negative errors, which first appear close to the wall at $x_K = 100$ mm and spread over the entire range of d^+ investigated. For $x_K \geqslant 215$ mm a region with uniform pressure exists upstream of the test station (see figure 5) and the errors decay. The decay is independent of d^+ as shown in figure 9. The idea that the universal part of the boundary layer reforms at the wall and diffuses into the boundary layer obviously does not hold for the constant-pressure region (215 mm $\leqslant x_K \leqslant$ 350 mm) of the present investigation. The momentum thickness δ^{**} at x_K equals about 3.6 mm, which leads to a decay length of about 40 δ^{**}.

The corresponding velocity distributions are shown in figure 10, measured with the 0.5 mm Preston tube moved away from the wall. The only correction applied was that of McMillan (1956) of the distance y from the wall. There are regions where the velocities are lower than predicted by the law of the wall. These regions correspond well with the negative errors shown in figure 8. These results are fully confirmed by an independent investigation on a plane wall reported by Zurfluh (1984). As this investigation served a different purpose, no systematic variations of the pressure gradient were made. Therefore only one typical result is shown in figure 11 and 12. The Preston-tube error and the pressure distribution are comparable with the case with $x_K = 100$ mm in figure 8, and the trend with x_K shown in figure 8 could be confirmed with different pressure distributions.

The velocity profile (figure 12) was measured with a hot wire. It also shows a

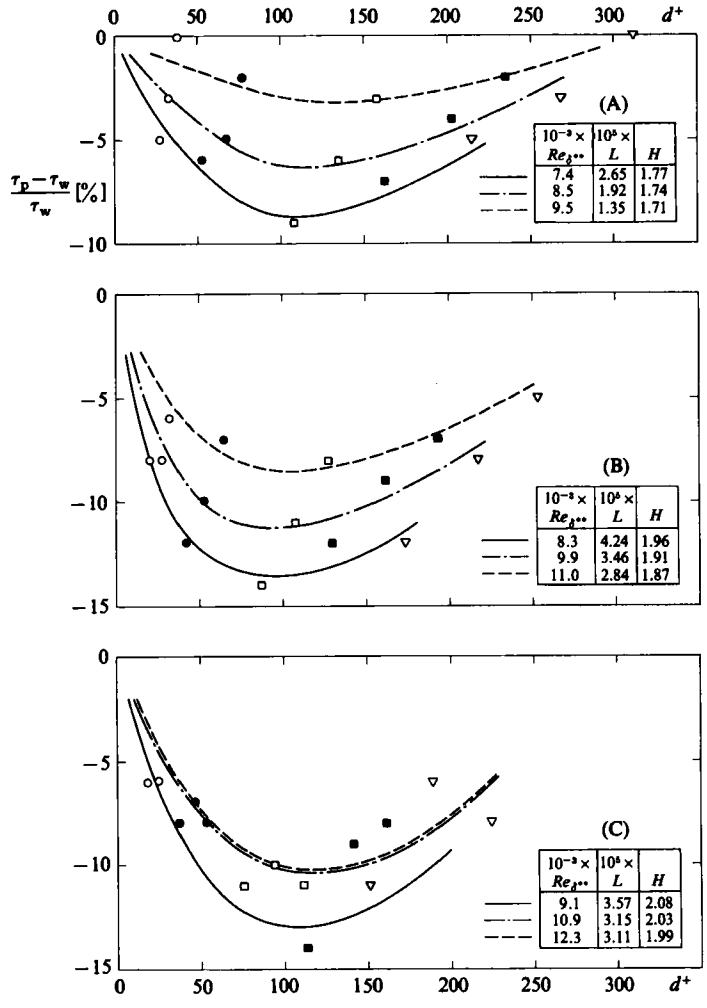

FIGURE 7. Errors of Preston-tube readings at $dp/dx = 0$ and $d^2p/dx^2 = 0$ (see figure 5). ○, $d = 0.5$ mm; ●, 1 mm; □, 2 mm; ■, 3 mm; ▽, 4 mm. ——, $q_D = 1000$ N/m²; —·—, 1500 N/m²; – – –, 2000 N/m². (A) $x_K = 215$ mm; (B) 265 mm; (C) 315 mm.

velocity defect close to the wall which corresponds with the negative Preston-tube errors in figure 11. Near $y^+ = u_\tau y/\nu = 200$ a crossover with the log law is seen and for higher y^+ the expected positive deviation is recorded, again in agreement with the Preston-tube readings in figure 11.

4. Discussion

It is generally agreed that in a turbulent boundary layer with $dp/dx = 0$, there exists a layer close to the wall with universal relations between the velocity $u = u^+ u_\tau$, the velocity fluctuations $(\overline{u_i'^2})^{\frac{1}{2}} = u_i^+ u_\tau$ and the wall distance $y = y^+ \nu/u_\tau$ of the form

$$u^+ = f(y^+), \tag{4.1}$$

$$u_i^+ = g_i(y^+). \tag{4.2}$$

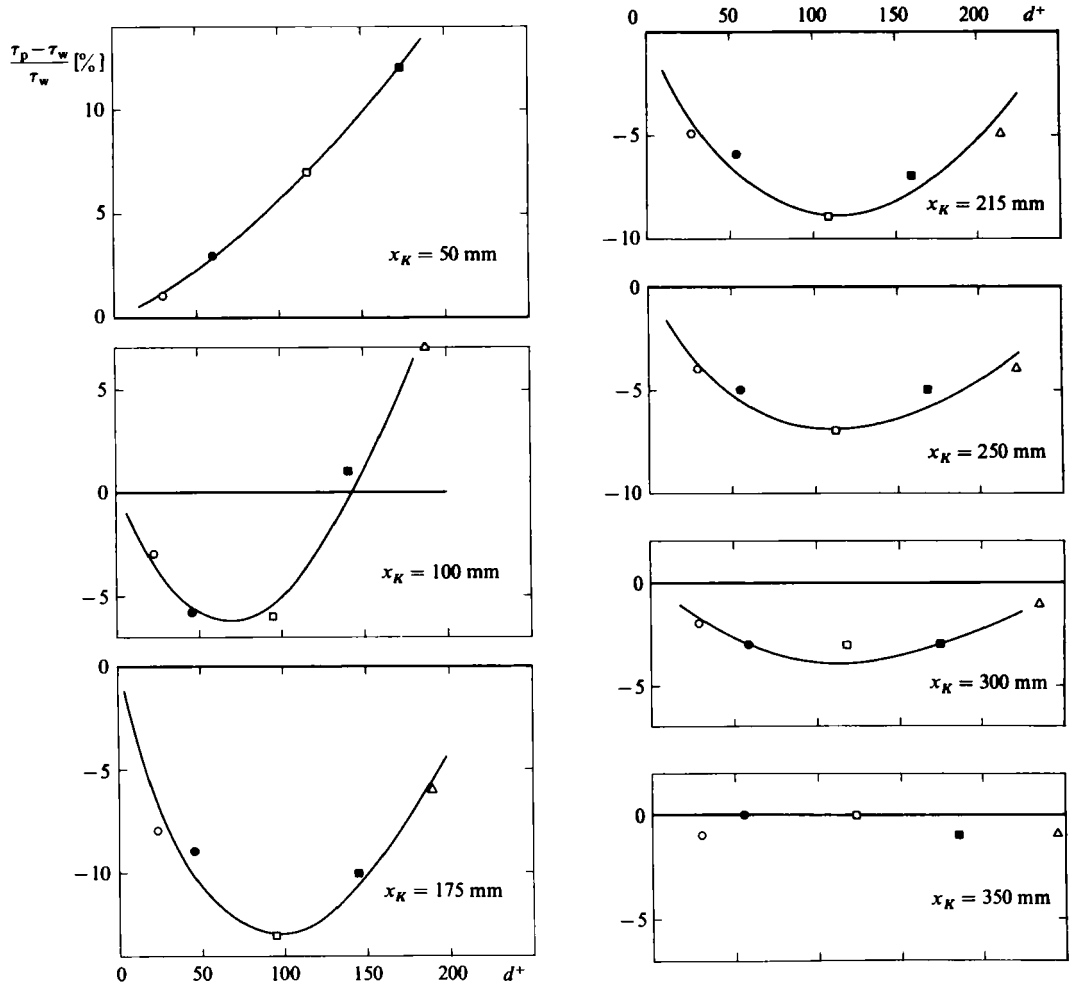

FIGURE 8. Development of the Preston-tube error along the boundary layer, insert (A), $q_D = 1000$ N/m². ○, $d = 0.5$ mm; ●, 1 mm; □, 2 mm; ■, 3 mm; △, 4 mm.

Well-known expressions for (4.1) are

$$u^+ = y^+, \tag{4.3}$$

$$u^+ = \frac{1}{k}\ln y^+ + A. \tag{4.4}$$

As long as (4.1) and (4.2) hold, a universal relation exists between the reading Δp of a Preston tube and the wall shear stress τ_w as demonstrated by Preston (1954).

A pressure gradient complicates the flow considerably as, in principle, the whole upstream pressure distribution must be taken into account. For the present purpose the influence of the pressure gradient on the layer close to the wall (say $y^+ \leqslant 200$) and the parameters that characterize this influence are of main interest. Of the large number of important contributions only a few can be quoted here.

Clauser (1954) introduced the concept of an equilibrium boundary layer with a logarithmic layer (4.4), close to the wall and a defect law

$$\frac{u_e - u}{u_\tau} = f\left(\frac{y}{\delta}; \frac{\delta'}{\tau_w}\frac{dp}{dx}\right), \tag{4.5}$$

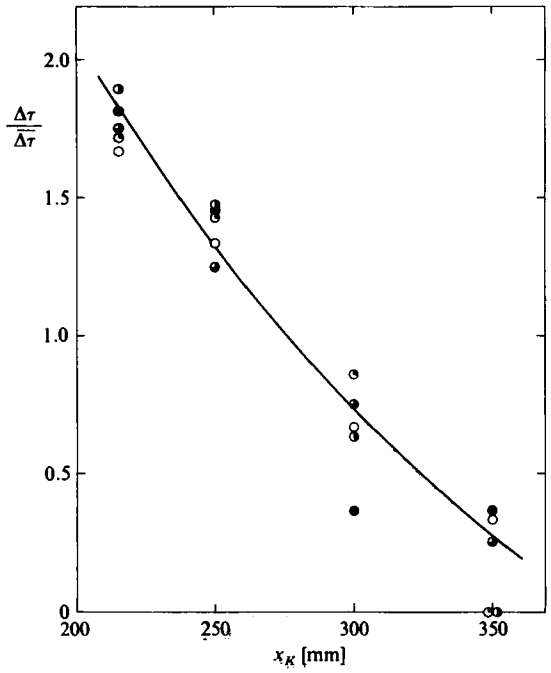

FIGURE 9. Decay of the error for $p(x) =$ constant. ○, $d^+ \approx 30$; ◔, 60; ◑, 120; ◕, 180; ●, 240; $\Delta\tau = \tau_p(d, x_K) - \tau_w(x_K)$; $\overline{\Delta\tau}$ is the average of $\Delta\tau$ over x_K.

where u_e is the velocity at the outer edge of the boundary layer and δ' is a lengthscale related to the boundary-layer thickness δ. In later work δ' has often been replaced by the displacement thickness δ^*. Special pressure distributions, described by one constant parameter

$$C = \frac{\delta^*}{\rho u_\tau^2}\frac{\mathrm{d}p}{\mathrm{d}x}, \tag{4.6}$$

will therefore lead to similar velocity profiles in the outer layer described by (4.5).

For laminar flow this idea leads to the well-known Falkner–Scan solution but for turbulent flow there exists a second lengthscale ν/u_τ which limits the concept of similarity for the whole boundary layer. Recent surveys of this type of flow are given by Yaglom (1979) and by Schofield (1981). The other limit considers a flow suddenly disturbed by the application or removal of a pressure gradient. The pertinent literature for this case is reviewed by Smits & Wood (1985).

Coles (1956) introduced his law of the wake, which is not restricted to a constant parameter C. It was used in the form

$$u^+ = \frac{1}{k}\ln y^+ + A + \frac{2\Pi}{k}\sin^2\left(\frac{\pi}{2}\frac{y}{\delta}\right), \tag{4.7}$$

with $k = 0.41$ and $A = 5$, as frame for the presentation of the data at the 1968 Stanford Conference (Coles & Hirst 1968).

Townsend (1961) used the term 'equilibrium layer' for a region close to the wall in which the production and dissipation of turbulent energy are in equilibrium. For an equilibrium layer with a linear shear-stress distribution of the form

$$\tau = \tau_w + \alpha y \tag{4.8}$$

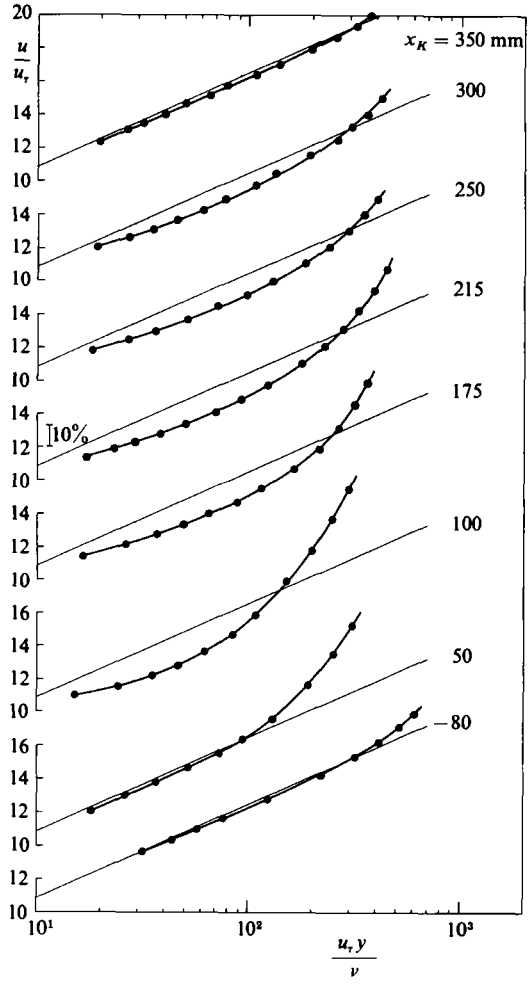

FIGURE 10. Velocity profiles for Insert (A), $q_D = 1000$ N/m². ——, $u/u_\tau = 5.5 \log_{10} (u_\tau y/\nu) + 5.45$.

he derives an expression for the velocity distribution that reads in the present nomenclature for $\alpha \geqslant 0$

$$u^+ = \frac{1}{k} \ln\left[\frac{(1+Ty^+)^{\frac{1}{2}}-1}{(1+Ty^+)^{\frac{1}{2}}+1}\frac{4}{T}\right] + A + \frac{2(1-B)}{k}[(1+Ty^+)^{\frac{1}{2}}-1], \tag{4.9}$$

with $B \approx 0.2$ and $T = \nu(\partial\tau/\partial y)/\rho u_\tau^3$.

For $T \to 0$ (4.9) reduces to (4.4) while for $\alpha y \gg \tau_w$ ($Ty^+ \gg 1$) it reduces to the well-known half-power law

$$u = \text{const}\ (\alpha y)^{\frac{1}{2}} + \text{const}. \tag{4.10}$$

It is very difficult to determine experimentally $\partial\tau/\partial y$ near the wall. The momentum equation is often used to replace $\partial\tau/\partial y$ by $\mathrm{d}p/\mathrm{d}x$ as $\mathrm{d}p/\mathrm{d}x$ can easily be measured. The assumption $u^+ = f(y^+)$ leads, without further assumptions, to

$$\frac{\partial\tau}{\partial y} = \frac{\mathrm{d}p}{\mathrm{d}x} + \rho u^{+2} u_\tau \frac{\mathrm{d}u_\tau}{\mathrm{d}x}, \tag{4.11}$$

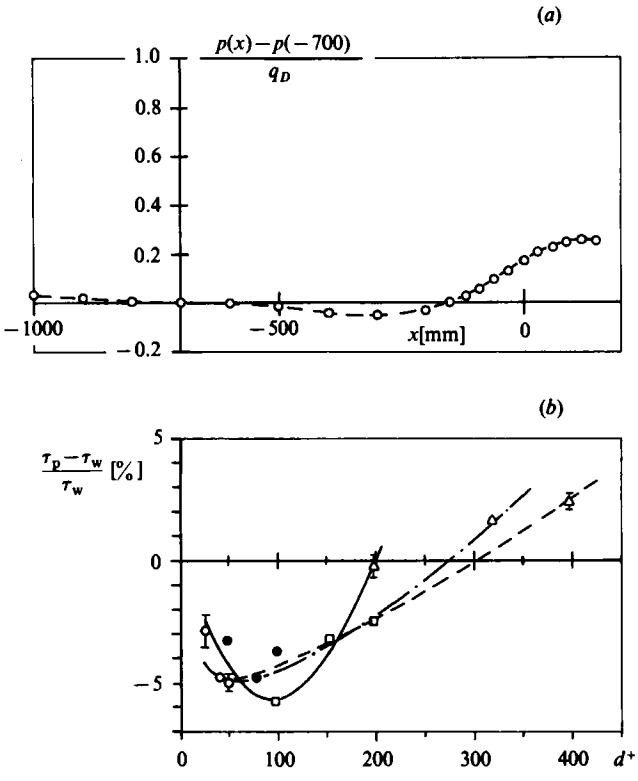

FIGURE 11. (*a*) Pressure distribution for $q_D = 1500$ N/m², boundary-layer trip at $x = -1427$ mm, balance at $x = 0$. Results from Zurfluh (1984). (*b*) Preston-tube error. ——, $q_D = 500$ N/m², $P = 1.65 \times 10^{-2}$, $P' = -2.2 \times 10^{-6}$, $L = -5.05 \times 10^{-5}$; — · —, $q_D = 1500$ N/m², $P = 1.19 \times 10^{-2}$, $P' = -1.1 \times 10^{-6}$, $L = -3.13 \times 10^{-5}$; – – –, $q_D = 2500$ N/m², $P = 1.03 \times 10^{-2}$, $P' = -0.7 \times 10^{-6}$, $L = -2.57 \times 10^{-5}$. ○, $d = 0.5$ mm; ●, 1 mm; □, 2 mm; △, 4 mm.

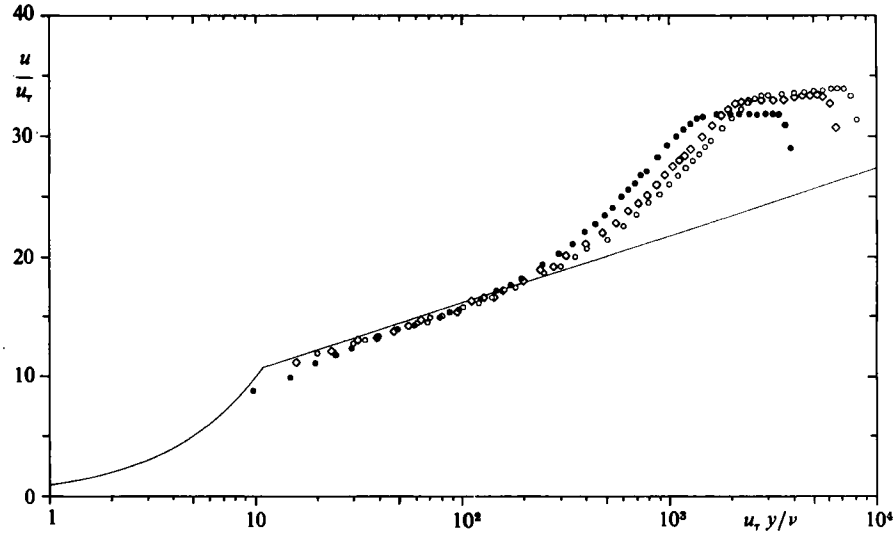

FIGURE 12. Velocity distribution at the location of the balance. ●, $q_D = 500$ N/m²; ◇, 1500 N/m²; ○, 2500 N/m².

If the wall scales ν/u_τ and u_τ are introduced into (4.11) the result is

$$T = P + Lu^{+2} \tag{4.12}$$

with the new parameters

$$P = \frac{\nu}{\rho u_\tau^3}\frac{\mathrm{d}p}{\mathrm{d}x} \tag{4.13}$$

and

$$L = \frac{\nu}{u_\tau^2}\frac{\mathrm{d}u_\tau}{\mathrm{d}x}. \tag{4.14}$$

The parameter P appears in most theories that treat turbulent boundary layers subject to pressure gradients. The influence of the inertia term (Lu^{+2} in (4.12)), on the other hand, is often neglected. For the present experiments with strong changes of P with x it seems likely that the inertia terms are important and L will thus be retained as a parameter.

Perry, Bell & Joubert (1966) suggested a region III adjacent to the logarithmic region with a relation

$$u^+ = K(Py^+)^{\frac{1}{2}} + \frac{1}{k}\ln\left(\frac{0.19}{P}\right) + A, \tag{4.15}$$

with $K = 4.16$ and with a junction between (4.4) and (4.15) at

$$y_c^+ = \frac{1.41}{P}. \tag{4.16}$$

Kader & Yaglom (1978) modify the half-power law (4.15) by assuming $K = K(P)$.

McDonald (1969) took into account the above-mentioned difference between $\mathrm{d}p/\mathrm{d}x$ and $\partial\tau/\partial y$ and determined expressions for $u^+(y^+)$. All these theories predict that $u^+(y^+)$ is larger than indicated by (4.4) if $P > 0$, and McDonald (1969) showed that realistic differences between $\mathrm{d}p/\mathrm{d}x$ and $\partial\tau/\partial y$ do not change this result.

Stratford's (1959) experiments with vanishing wall shear stress (and thus u_τ) showed the need for a modification of the velocity scale close to separation. His result is

$$u = \frac{2}{k}\left(\frac{1}{\rho}\frac{\mathrm{d}p}{\mathrm{d}x}y\right)^{\frac{1}{2}}. \tag{4.17}$$

Introducing a velocity scale

$$u_p = \left(\frac{\delta'}{\rho}\frac{\mathrm{d}p}{\mathrm{d}x}\right)^{\frac{1}{2}} \tag{4.18}$$

into (4.17) leads to the non-dimensional form

$$\frac{u}{u_p} = \frac{2}{k}\left(\frac{y}{\delta'}\right)^{\frac{1}{2}}.$$

Any length δ' can be chosen but it is reasonable to assume that δ' is a fraction of the boundary-layer thickness δ. Mellor & Gibson (1966) used $\delta' = \delta^*$ in (4.18) while Kader & Yaglom (1978) suggested $\delta' = \delta$. For the present case it is sufficient to note that the new velocity scale does not introduce a new parameter as $(u_p/u_\tau)^2$ equals Clauser's parameter C in (4.6). Schofield (1981) suggests a velocity scale based on the maximum shear stress τ_m in the layer. This suggestion leads to an additional parameter $\tau_\mathrm{m}/\tau_\mathrm{w}$ which looks promising for theoretical work but which cannot be used to correlate the present experiments as τ_m was not measured.

It is obvious, and mentioned by McDonald (1969) and Kader & Yaglom (1978) among others, that the higher derivatives of $p(x)$ will have some influence on the flow field but it seems much more difficult to take this effect into account in a theoretical approach. In spite of that the parameter

$$P' = \frac{\nu^2}{\rho u_\tau^4} \frac{\mathrm{d}^2 p}{\mathrm{d}x^2} \tag{4.19}$$

was suggested by Frei & Thomann (1980) and used to correlate the measurements. Finally, the shape factor

$$H = \delta^*/\delta^{**} \tag{4.20}$$

was determined as it will appear in (4.21) and (4.22) for the wall shear stress.

The reading Δp of a Preston tube can be reduced to a velocity by introducing a displacement of its effective centre to $\frac{1}{2}Kd$ as suggested by Patel (1965). For a boundary layer with constant pressure $K = K(d^+)$. Patel determined K by comparing $u = (2\Delta p/\rho)^{\frac{1}{2}}$ from his measured Δp with $u(\frac{1}{2}Kd)$ that was predicted with equations similar to (4.3) and (4.4). A figure close to McMillan's (1956) 1.3 resulted for K. Similar ideas led Brown & Joubert (1969) to the prediction that the error of a Preston tube should vanish for $d^+ < y_c^+$ with y_c^+ given by (4.16) and that the error should be a function of $d^+/y_c^+ = d^+P/1.41$ as long as the half-power law is valid. A great number of papers that predict Preston-tube errors have been based on similar ideas.

It is well known that the reading of a Pitot tube is influenced by the turbulent velocity fluctuations. Corrections are suggested by Hinze (1959, p. 136) which show that the reading increases with increasing turbulence intensity as long as the probe is fairly insensitive to crossflow, which is the case for the Preston-tube geometry.

The experiments of Simpson, Strickland & Barr (1977), of Pozzorini (1976) and of numerous other investigators show that the intensity of the fluctuations with respect to the local velocity are increased by an adverse pressure gradient.

The reading Δp of a Preston tube subject to a constant wall shear stress should therefore increase if an adverse pressure gradient is applied as, first, the mean velocity $u^+(y^+)$ is increased above the law of the wall and, second, the fluctuations are increased. The calibration curve for a Preston tube at constant pressure should therefore indicate too high a wall shear stress, which is in contrast to the negative errors shown in figures 4, 7 and 8. These negative errors indicate therefore significant velocity defects for y^+ as low as 10, which is in agreement with the velocity profiles in figure 10. These negative deviations might be fictitious and caused by errors of the τ_w measurement. This, however, is very unlikely for several reasons. First, it was shown by Hirt, Zurfluh & Thomann (1986) that errors introduced by comparable pressure gradients are well below 1 %; second, the errors are also observed in the constant-pressure part (see figures 8 and 9) where there is no reason to doubt the reading of the balance; and, finally, similar negative errors were also observed by Zurfluh (1984), as described at the end of §3.

Finally, an attempt was made to correlate the errors with the local parameters P, P', L and H defined in (4.13), (4.14), (4.19) and (4.20). The parameters C, P and P' that are based on $p(x)$ fail to correlate the results shown in figure 4 and 7 as $\mathrm{d}p/\mathrm{d}x$ vanishes in both cases while $\mathrm{d}^2p/\mathrm{d}x^2$ vanishes in the second one. Neither can they describe the decay of the errors in the region with constant pressure in figures 8 and 9 as they vanish there. More promising in this respect are the parameters L and H.

The distribution of all parameters along x is compared in figure 13 with the error of the Preston tube with $d = 2$ mm ($d^+ \approx 100$). This tube was chosen as the errors

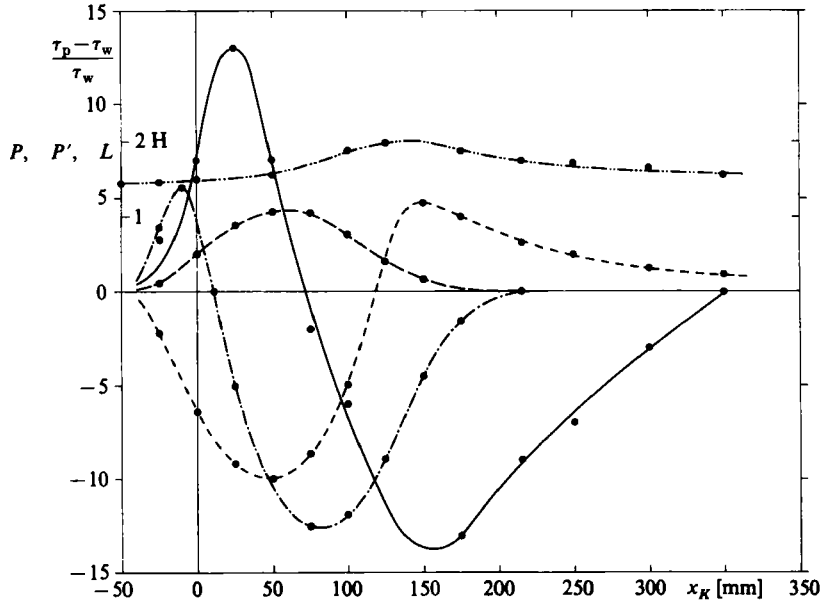

FIGURE 13. Parameters and Preston-tube error for insert (A), $q_D = 1000$ N/m², $d = 2$ mm, $d^+ \approx 100$, ——, $10^2 \times (\tau_p - \tau_w)/\tau_w$; — —, $10^2 \times P$; — · —, $10^6 \times P'$; – – –, $10^5 \times L$; — · · —, H.

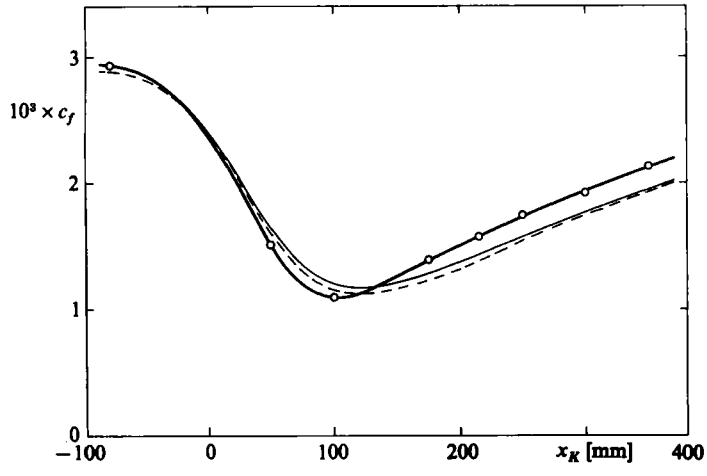

FIGURE 14. Comparison of (4.21) and (4.22) with experiments, insert (A), $q_D = 1000$ N/m². —○—, measured shear stress; ——, (4.21); – – –, (4.22).

have a maximum near $d^+ = 100$ in the present case. It is again seen that no single parameter correlates with the error. Similar results are found for $d^+ = 25$.

The measured wall shear stress is compared in figure 14 with the equation

$$c_f = \frac{2\tau_w}{\rho u_e^2} = 0.246 \cdot 10^{-0.678H} \left(\frac{u_e \delta^{**}}{\nu}\right)^{-0.268} \tag{4.21}$$

suggested by Ludwieg & Tillmann (1949). A similar equation that should be valid

closer to separation was suggested by Fernholz (1964). It reads, with the present notation,

$$c_f = 0.0580\left[\log_{10}\frac{8.05}{H^{1.818}}\right]^{1.705}\left(\frac{u_e\,\delta^{**}}{\nu}\right)^{-0.268} \tag{4.22}$$

It is interesting to note that the predictions of (4.21) and (4.22) are similar to the Preston-tube results. For $x_K < 100$ mm the surface shear stress is overestimated by about 10 % while it is underestimated by about the same amount for $x_K > 200$ mm.

5. Conclusions

Sudden application and removal of adverse pressure gradients generated boundary layers far from equilibrium. The Preston-tube calibration for a flat plate leads to considerable errors for boundary layers of this type. Errors of $-10\,\%$ result for d^+ as low as 10 (see figure 4) in regions where $\mathrm{d}\tau_w/\mathrm{d}x > 0$. Indirect methods used to determine the wall shear stress (heat-transfer gauges, surface fences, etc.) should therefore not extend beyond $y^+ = 3$ for similar pressure distributions.

Negative errors of the Preston tube (low readings) indicate velocity profiles lower than the logarithmic law, (4.4), even in positive pressure gradients. This is confirmed with velocity measurements.

No local parameters were found that could describe the Preston-tube correlations.

The Ludwieg & Tillmann relation (4.21) agreed to within $\pm 10\,\%$ with the present measurements in spite of the severe pressure gradients.

REFERENCES

Brown, K. C. & Joubert, P. N. 1969 The measurement of skin friction in turbulent boundary layers with adverse pressure gradients. *J. Fluid Mech.* **35**, 737–757.

Clauser, F. H. 1954 Turbulent boundary layers in adverse pressure gradients. *J. Aero. Sci.* **21**, 91–108.

Coles, D. 1956 The law of the wake in the turbulent boundary layer. *J. Fluid Mech.* **1**, 191–226.

Coles, D. & Hirst, E. A. 1968 *AFOSR–IFP Stanford Conf. on Turbulent Boundary Layer Prediction*, vol. 2.

Fernholz, H. 1964 Halbempirische Gesetze zur Berechnung turbulenter Grenzschichten nach der Methode der Integralbedingungen. *Ing. Archiv* **33**, 384–395.

Frei, D. & Thomann, H. 1980 Direct measurements of skin friction in a turbulent boundary layer with a strong adverse pressure gradient. *J. Fluid Mech.* **101**, 79–95.

Hinze, J. O. 1959 *Turbulence*. McGraw-Hill.

Hirt, F. 1984 Anzeige des Prestonrohres im Druck-gradient. *Diss. ETH Nr.* 7531.

Hirt, F., Zurfluh, U. & Thomann, H. 1986 Skin friction balances for strong pressure gradients. *Experiments in Fluids* **4**, 296–300.

Kader, B. A. & Yaglom, A. M. 1978 Similarity treatment of moving-equilibrium turbulent boundary layers in adverse pressure gradients. *J. Fluid Mech.* **89**, 305–342.

Ludwieg, H. & Tillmann, W. 1949 Untersuchungen über die Wandschubspannung in turbulenten Reibungsschichten. *Ing. Archiv* **17**, 228–299.

McDonald, H. 1969 The effect of pressure gradient on the law of the wall in turbulent flow. *J. Fluid Mech.* **35**, 311–336.

McMillan, A. F. 1956 Experiments on pitot tubes in shear flow. *ARC R & M*, no. 3028.

Mellor, G. L. & Gibson, D. M. 1966 Equilibrium turbulent boundary layers. *J. Fluid Mech.* **24**, 225–253.

PATEL, V. C. 1965 Calibration of the Preston tube and limitations on its use in pressure gradients. *J. Fluid Mech.* **23**, 185–208.

PERRY, A. E., BELL, J. B. & JOUBERT, P. N. 1966 Velocity and temperature profiles in adverse pressure gradient turbulent boundary layers. *J. Fluid Mech.* **25**, 299–320.

POZZORINI, R. 1976 Das turbulente Strömungsfeld in einem langen Kreiskegel Diffusor. *Diss. ETH*, nr. 5646.

PRESTON, J. H. 1954 The determination of turbulent skin friction by means of Pitot tubes. *J. R. Aeron. Soc.* **58**, 109–121.

SCHOFIELD, W. H. 1981 Equilibrium boundary layers in moderate to strong adverse pressure gradients. *J. Fluid Mech.* **113**, 91–122.

SIMPSON, R. L., STRICKLAND, J. H. & BARR, P. W. 1977 Features of a separating turbulent boundary layer in the vicinity of separation. *J. Fluid Mech.* **79**, 553–594.

SMITS, A. J. & WOOD, D. H. 1985 The response of turbulent boundary layers to sudden perturbations. *Ann. Rev. Fluid Mech.* **17**, 321–358.

STRATFORD, B. S. 1959 An experimental flow with zero skin friction throughout its region of pressure rise. *J. Fluid Mech.* **5**, 17–35.

TOWNSEND, A. A. 1961 Equilibrium layers and wall turbulence. *J. Fluid Mech.* **11**, 97–120.

YAGLOM, A. M. 1979 Similarity laws for constant-pressure and pressure-gradient turbulent wall flows. *Ann. Rev. Fluid Mech.* **11**, 505–540.

ZURFLUH, U. E. 1984 Experimentelle Bestimmung der Wandschubspannung in turbulenten Grenzschichten. *Diss. ETH Nr.* 7528.